Corrosion assessment of Zn-rich epoxy primers with carbon nanotube additions in an electrolyte with a bacteria consortium

HOMERO Castaneda-Lopez[1*], Israel Barraza[1], Monica GAlicia[2], Violeta Valencia[2]

[1]Texas A&M University, United States, [2]Universidad Autónoma de Ciudad Juárez, Mexico

Submitted to Journal:
Frontiers in Materials

Specialty Section:
Environmental Materials

Article type:
Original Research Article

Manuscript ID:
483949

Received on:
09 Jul 2019

Revised on:
25 Oct 2019

Frontiers website link:
www.frontiersin.org

Conflict of interest statement

The authors declare that the research was conducted in the absence of any commercial or financial relationships that could be construed as a potential conflict of interest

Author contribution statement

The authors contribution is included in this work and was essential to the completion and submission.

Keywords

zinc-rich epoxy coatings, , multiwalled carbon nanotubes, biocorrosion, sulfate-reducing microorganisms, Multifunctional coatings

Abstract

Word count: 180

Multifunctional coatings for corrosive environments have been developed to include two basic principle protection mechanisms: a barrier mechanism acting as a mass transfer process blocker, and cathodic protection mechanism acting as a charge transfer process promoter. Both mechanisms were assessed for Zinc-Rich Epoxy (ZRE) coatings in the presence of Carbon Nanotubes (CNTs) and exposure to a bioelectrolyte in order to study the evolution process during microbial corrosion conditions. The purpose of this study is to characterize in a comprehensive experimental platform the electrochemical response of a dual-protection zinc epoxy coating with different ratios of additive carbon nanotubes to active zinc particles upon exposure to a sulfate reducing consortium. Carbon nanotubes addition was found to affect both the prevailing mechanism at the coating interfaces and the formation of a biofilm at the coating surface that influenced the relatively dominance of the barrier protection mechanism. These multifunctional coatings with active particles could help to balance the charge transfer efficiency in terms of the sacrificial of zinc and barrier mechanisms, which influence biofilm formation and have potential consequences for biocorrosion on carbon steel.

Contribution to the field

This work aims to determine the electrochemical behavior of a Zn-rich primer with MWCNTs additions in an electrolyte containing an SRB consortium.. A few studies have evaluated Zn-rich epoxy primers in media containing sulfate reducing bacteria but to the best of our knowledge no studies have investigated Zn-rich primers with MWCNTs added to their matrix in an environment including a sulfate reducing consortium.

Ethics statements

Studies involving animal subjects

Generated Statement: No animal studies are presented in this manuscript.

Studies involving human subjects

Generated Statement: No human studies are presented in this manuscript.

Inclusion of identifiable human data

Generated Statement: No potentially identifiable human images or data is presented in this study.

Data availability statement

Generated Statement: All datasets generated for this study are included in the manuscript/supplementary files.

Corrosion assessment of Zn-rich epoxy primers with carbon nanotube additions in an electrolyte with a bacteria consortium

H. Castaneda[1*], M. Galicia[2]

[1*]Department of Materials Science and Engineering, Texas A&M University, College Station, TX, USA
[2]Instituto de Ciencias Biomédicas, Departamento de Ciencias Químico Biológicas, Universidad Autónoma de Ciudad Juárez, Ciudad Juárez, CH, México.
.
* Correspondence:
Homero Castaneda
hcastaneda@tamu.edu

Keywords: zinc-rich epoxy coatings, carbon nanotubes, biocorrosion, sulfate-reducing microorganisms.

Abstract

Multifunctional coatings for corrosive environments have been developed to include two basic principle protection mechanisms: a barrier mechanism acting as a mass transfer process blocker, and cathodic protection mechanism acting as a charge transfer process promoter. Both mechanisms were assessed for Zinc-Rich Epoxy (ZRE) coatings in the presence of Carbon Nanotubes (CNTs) and exposure to a bioelectrolyte in order to study the evolution process during microbial corrosion conditions. The purpose of this study is to characterize in a comprehensive experimental platform the electrochemical response of a dual-protection zinc epoxy coating with different ratios of additive carbon nanotubes to active zinc particles upon exposure to a sulfate reducing consortium. Carbon nanotubes addition was found to affect both the prevailing mechanism at the coating interfaces and the formation of a biofilm at the coating surface that influenced the relatively dominance of the barrier protection mechanism. These multifunctional coatings with active particles could help to balance the charge transfer efficiency in terms of the sacrificial of zinc and barrier mechanisms, which influence biofilm formation and have potential consequences for biocorrosion on carbon steel.

1. Introduction

Most coatings used for microbiologically induced corrosion (MIC) in industry are designed to provide an effective barrier to inhibit corrosion processes and/or provide a biocidal effect. These coatings are synthetized using organic, inorganic, and hybrid approaches. Organic coatings have been demonstrated to provide an effective physical barrier in a variety of aggressive conditions (Abdolahi et al., 2014, Deflorian et al., 2005, Fedel et al., 2019). However, when exposed to anoxic conditions such as those prevailing in seawater or oil and gas pipelines, some of these coatings

degrade faster upon exposure to either a bacterial consortium or a specific strain of microbial attack (Enning and Garrelfs, 2014).

Unfortunately, inorganic and hybrid protective coatings on steel have also been proven to degrade when exposed to MIC in such anoxic conditions (Abdolahi et al., 2014; Enning and Garrelfs, 2014; Ciubotariu et al., 2015). Environmentally friendly coatings are being developed to improve their physicochemical properties to resist microbiological attack, either in aerobic or anaerobic conditions, while avoiding toxicity to the environment from the inherently toxic formulations of some coatings.

Recent coating research has investigated nano-architected sacrificial coatings as a new technology with dual protection mechanisms. The first is galvanic or cathodic protection, which is achieved by integrating electrochemically active particles into the organic coating matrix. The second protection mechanism is the classical barrier effect offered by a polymeric matrix. The addition of nanostructures such as carbon nanotubes (CNTs) can enhance both properties by influencing the interconnectivity of active particles and filling the voids created during synthesis of the coating in the polymeric matrix, as noted by Cubides and Castaneda (Cubides and Castaneda, 2016).

Zn-rich epoxy primers have shown excellent results and have been used by the industry since the 60's and 70's (Weinell and Rasmussen, 2007). The mechanisms of corrosion protection in the Zn-rich epoxy primers include a galvanic effect due to metallic zinc dissolution, as well as a barrier effect resulting not only from the epoxy resin but also via the formation of Zn and Fe products (Deflorian et al., 2005, Weinell and Rasmussen, 2007). However, a balance must be considered in the formulation in order to assure cathodic protection for an extended time. A load of 90 wt.% of Zn particles may be beneficial for the charge transfer process (Park and Shon, 2015). However, that amount can reduce substrate adhesion and cause problems with the spraying application related to the high viscosity and poor dispersion of zinc particles (Park and Shon, 2015). Hence, research has sought to decrease the percentage of Zn load while retaining the connection among the particles and maintaining or increasing mechanical coating properties (Weinell and Rasmussen, 2007; Park and Shon, 2015; Jeon et al., 2013).

Weinell and Rasmussen (Weinell and Rasmussen, 2007) noted that different pigments, such as thixotropic agents, can be added to the epoxy matrix of coatings to prevent zinc precipitation. The authors incorporated colored pigments to differentiate between steel substrate and the greyish Zn primer, adding oil-absorbing pigments to decrease the Zn load while maintaining the same level of cathodic protection. Park and Shon suggested the addition of multiwalled carbon nanotubes (MWCNTs) to a maximum load of 0.6 wt.%, which resulted in improved conductivity, adhesion strength, and corrosion protectiveness as the MWCNTs increased from 0 to 0.25 wt.% (Park and Shon, 2015). Similarly, the addition of MWCNTs in an epoxy coating provided greater adhesion strength, transport behavior, and hydrophobicity as the MWCNT concentration increased from 0 to 0.5 wt.% (Jeon et al., 2013).

The microbiological environment and underlying mechanisms have not been extensively explored in coating studies of Zn-rich epoxy primers. A few studies have evaluated Zn-rich epoxy primers in media containing sulfate reducing bacteria (Wang et al., 2012; Liu et al., 2007), but to the best of our knowledge no studies have investigated Zn-rich primers with MWCNTs added to their matrix in an environment including a sulfate reducing consortium.

This work aims to determine the electrochemical behavior of a Zn-rich primer with MWCNTs additions in an electrolyte containing an SRM consortium. Electrochemical techniques were used to elucidate the interfacial mechanisms. We used electrochemical impedance spectroscopy as a

primer technique to characterize the mechanisms presented at different interfaces formed in the system, and the results were analyzed using electrical analog element coupled with high-resolution surface techniques. Different CNTs compositions were used to support the influence of the mechanism's dominance based on the corrosion control method.

2. Materials and Methods

2.1 Microbial culture

The consortium of sulfate reducing bacteria (sulfate reducing microorganisms) used in this study was collected with an in-line inspection tool used for internal inspection in pipelines (the so-called smart 'PIGS"). The sample consortium was inoculated in ATCC1250 modified Baar's medium for Sulfate Reducers with NaCl (2.5 wt.%) [ATTC®]. The pH value was adjusted to 7.2 under de-aeration by applying nitrogen to the electrolyte. The medium was autoclaved at 120°C for 15 min. The SRM consortium was incubated at 37°C.

2.2 Multifunctional Coatings.

The Zn-rich epoxy primers and multiwalled carbon nanotubes were supplied by Tesla NanoCoatings company. The epoxy resin (Tesla P1150ASAS) was mixed with CNTs at 1 and 2 wt.%. After the CNTs were completely dispersed in the epoxy resin through mechanical stirring according to a previously method (Cubides and Castaneda, 2016), Zn particles at 70 wt.% were slowly added while stirring the solution, and a hardener (Tesla P1150BSAS) was then poured in to a final weight ratio of 2:1 (epoxy resin-hardener). The 70 wt. % was used based on the previous work (Cubides and Castaneda, 2016) where is was demonstrated the Zn content was the most balanced for cathodic protection or sacrificial conditions. In addition, Zn-rich epoxy primer without CNTs was also used in this study. The coatings were air-sprayed onto UNS1008 steel plates. This procedure was performed previously (Cubides and Castaneda, 2016). Table 1 shows the different sample characteristics.

Table 1. Specifications of the different coating systems.

Table 1. Specifications of the different coating systems.

Coating	Zinc (wt.%)	(CNTs) (~wt.%)
ZnR	70	0
Zn-1CNT	70	1.0
Zn-2CNT	70	2.0

2.3 Electrochemical characterization.

A three-electrode electrochemical cell was used for the experimental characterization. The electrochemical cells were autoclaved. The working electrode was the multifunctional coating sample. The counter electrode was a platinum mesh, and the reference electrode was a saturated calomel electrode (SCE). The working electrodes and the reference and auxiliary electrode were sterilized with 70% ethanol and acetone and set under UV light and laminar flow. They were placed on a 25 mL electrochemical cell containing culture medium under N_2 gas injection before each experiment. It was conducted at 25°C. OCP was performed on prior EIS measurements during

a period of 10 minutes. EIS was performed in a frequency range of 100 KHz to 10 mHz with a ±10 mV peak-to-peak amplitude *vs.* the open circuit potential (OCP). All the tests were carried out in a potentionstat/galvanostat (VSP-300; Bio-Logic Science Instruments), using the software EC-Lab® V.10.32. All electrochemical experiments were performed in duplicate to ensure reproducibility of the electrochemical behavior.

2.4 SEM sample preparation.

Once the electrochemical test was completed, the samples were rinsed with PBS 1X (8.0 g of NaCl, 0.2 g of KCl, 1.4 g of $Na_2HPO_4 \cdot 2H_2O$, and 0.2 g of KH_2PO_4 per liter, pH= 7.2). Subsequently, the samples were fixed with glutaraldehyde 2.5% w/v in PBS for 2 h, with washing every 30 min. All fixation was conducted at room temperature. After fixation, the cells were washed twice in PBS and then re-suspended in sterilized ultrapure water to avoid salt crystallization during the drying process. The samples were dried for 24 h in a LABCONO Freeszone 6 lyophilizer. Finally, the samples were sputtered with silver particles and observed under a JSM-7000F/JOEL microscope through energy-dispersive spectroscopy (EDS).

3. Results and Discussion

3.1 Open circuit potential

The ZnR coating system shows the potential evolution influenced by different conditions and interfacial configurations such as the epoxy physical barrier, the galvanic phenomenon between zinc and steel, the physicochemical barrier of corrosion products, the concentration of Fe and Zn near the particle/coating or substrate/coating interfaces and inside the coating, amongst other factors, as described by Cubides (Cubides and Castaneda, 2016). The cathodic protection of steel has been established at ≤ -0.90 V *vs.* $Cu/CuSO_4$ (-0.826 *vs.* SCE) under anaerobic conditions (Schwerdtfeger, 1958; Guang et al., 2016; Liu and Cheng, 2017). This level is drawn as a dash line in Figure 1. At higher (more positive) potentials, barrier protection tends to be the dominant control mechanism, which may be associated with the epoxy-polymer and the corrosion products of Zn and/or Fe. The OCP monitoring of the AISI/SAE 1008 steel substrate and the multifunctional coatings under biotic conditions is shown in Figure 1. The OCP for the bare steel is more positive (passive region or protective layer region based on thermodynamics) than the cathodic potential criteria because the galvanic effect results in a negative potential value, in which the steel faces immune thermodynamic conditions. The OCP for the bare steel 1008 was determined in a test where the sample was kept in the culture medium in bacterial consortium conditions, and the steel potential was found to be influenced by the biofilm and corrosion products formed at the surface of the substrate. Classic work by Castaneda (Castaneda and Benetton, 2008) characterized mild steel in seawater in the presence of SRB, which resulted in positive potentials due to the combination of corrosion products and biofilm. Figure 1 shows the initiation and growth stages for the biofilm formation. At this respect, Castaneda marked 14 days for the initiation to biofilm growth transition, similar to this condition, where the OCP increases the magnitude following two weeks of exposure.

The Zn-rich primer (70 wt.% Zn) exposed to the bacteria consortium shows a potential oscillating within the barrier protection zone over the exposure time. This means that the Zn particles are

randomly distributed in the epoxy matrix with a connectivity between them that is insufficient to trigger the galvanic effect formation. There is a transient state during the first 10 days of exposure, and during this time, the potential values are in the barrier zone. This behavior is associated with water uptake in the coating and the formation of Zn products during the initial days of exposure. Finally, the potential is around the OCP of 1008 carbon steel in biotic conditions, but both experimental results are above the corrosion protection located in the barrier protection zone, and barrier zone dominance can result from the Zn-Fe corrosion products and/or biofilm formation to produce a blocking effect for the water uptake process.

At the early stage, the Zn-1CNT potential is located close to the cathodic protection zone for the first day. Following the negative potentials, a transient stage occurs during the next 10 days within the barrier protection area. The initial conditions could be the response of the bioelectrolyte wetting over the Zn particles and due to the interconnectivity among Zn particles and steel arising from the influence of MWCNTs or the cathodic protection effect; the potential between 4 and 10 days may be the result of Zn and/or Fe corrosion products acting as a barrier or passive particle state, which switches the system to prevail in more positive potentials. These latter compounds fill the porous surfaces within the coating structure, and the potential subsequently increases at day 2. The interaction between consortium/coating subsequently changes the quantity and morphology of the products, and the potential decreases at day 10. Eventually, the potentials reach approximately -0.680V *vs.* SCE in the barrier zone, 100 mV more negative than the ZnR sample. Subsequently, the potential remains stable at close to -0.680V *vs.* SCE. This latter effect could be due to the influence of the biofilm at the surface, in which the zinc ions inhibit the formation of the biofilm layer at initial conditions (Babich and Stotzky, 1978, Bong et al., 2010, Billanger et al., 2015, Tong et al., 2015), but the ions are depleted and the biofilm starts to grow over time to become more homogeneous and distributed compared with the 2CNT, and the magnitude of the potential becomes more negative than the ZnR sample to produce a less dominant barrier effect with the addition of 1CNT.

OCP for the Zn-2CNT sample are more negative than the threshold for the cathodic protection magnitude during the first 2 days. This behavior is associated with a greater MWCNTs concentration, resulting in better interconnection between the Zn/Zn electrical connection particles due to the CNT/Zn/CNT interconnectivity. This latter finding is confirmed in the cross-section SEM images. These potentials are more negative than the Zn-1CNT results. A transient potential state exists between days 3 and 10 of exposure. After 10 days, there are two transient states during the barrier protection zone and close to the cathodic protection threshold, one between 10 and 15 days and the other between 16 and 24 days. Finally, the potential keeps fluctuating in the barrier protection zone and reaches lower values than the OCP of carbon steel in biotic conditions. The potentials reveal the dominance of cathodic protection for this sample in different stages. Particle activation was promoted by the distribution of CNTs within the coating, and the products formed in the coating are not sufficiently compact to stop bioelectrolyte uptake within the coating, with the unstable biofilm leading to lower potential magnitudes. This may result from greater electrochemical activity among particle/coating interface. This latter result is evidence of a certain grade of galvanic effect, i.e., the system is at a lower potential than the value found for steel without coating due to reaction with the Zn particles. The presence of two increments may be due to the creation of products that fill the pores in the coating, with the decrease resulting from the particle layer and an interaction forming with an incipient heterogeneous biofilm. That is, zinc ion

formation inhibits biofilm growth and leads to various areas of biofilm depletion, thus affecting the morphology of these compounds over time and altering the distribution of the biofilm at the surface of the coating.

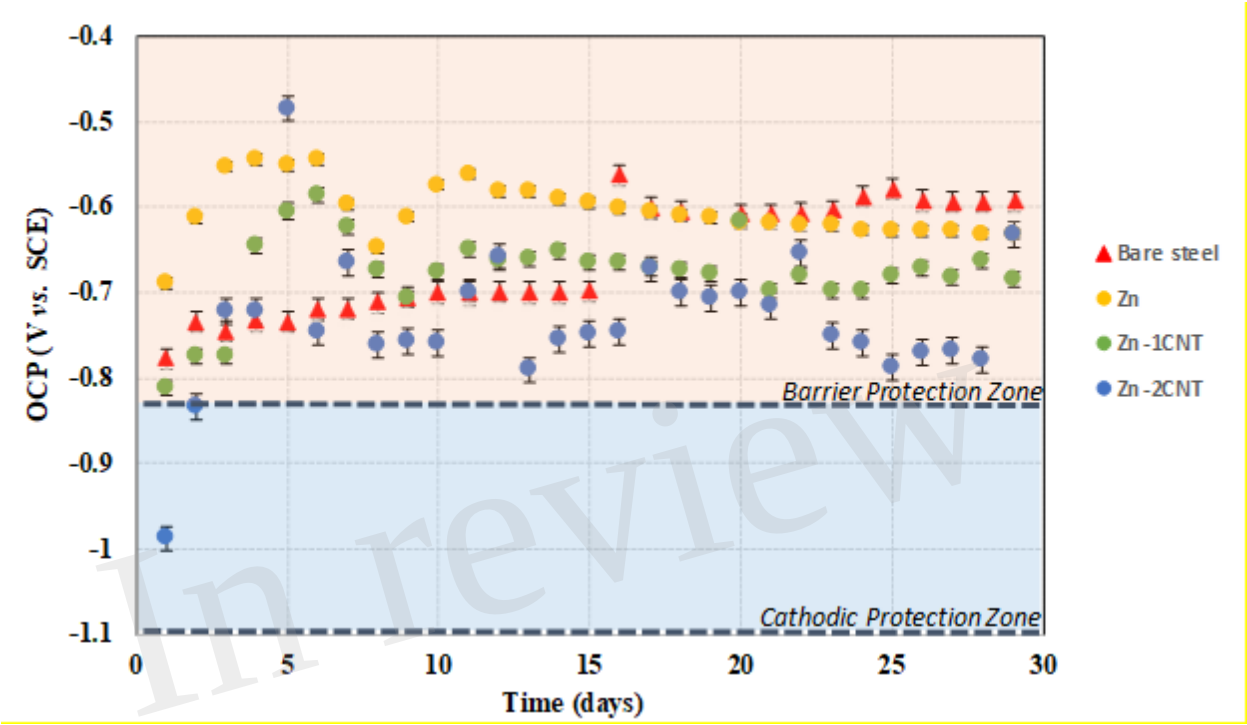

Fig. 1. OCP for bare steel and the three different multifunctional coatings under bioelectrolyte conditions

3.2 Qualitative analysis of impedance

Figure 2 shows the complex and phase angle diagrams for Bare steel and Zinc Rich Epoxy multifunctional coatings in SRM consortium environment.

The Nyquist representation for the AISI 1008 bare steel sample exposed to the biotic electrolyte is shown in Figure 2(a). The results show a loop with a large diameter characteristic of a capacitance and charge transfer process. The phase angle representation is illustrated in Figure 2(b). The medium frequency response is associated with capacitance (double layer) at the surface, whereas the response at low frequency is associated with the electrochemical reactions at the steel/electrolyte interface. On day 5, this system represents biofilm formation, and the corrosion products form an inorganic and organic mixing layer. At low frequencies, the magnitude of the semicircle's diameter is associated with the substrate/mixing layer/electrolyte interface. The magnitude for the biotic conditions results in a loop intercepting the locus point on the order of 12,000 Ω cm^2, whereas at 10 days, an increase in the loop diameter occurs, which may be associated with the accumulation of a mixing layer formed at the surface. At the surface, the number of active sites decreases, and the Rct increases, as previously described by Castaneda (Castaneda and Dominguez, 2008), with mild steel exposed to an SRM electrolyte during the first 2 weeks. At day 15, the impedance magnitudes begin to decrease, reflecting an activation

mechanism, and an increase in the number of active sites occurs at the metallic substrate/mixing layer interface. On day 20, the impedance lowers the magnitude for this sample, an effect associated with the active sites, owing to the charge transfer process. After 25 days, the contribution of two potential interfaces is revealed by two maximum points in the phase angle representation. At days 25, and 29, the active sites remain constant, owing to the maintenance of the impedance at low magnitudes and the formation of two separate contributions at the interface layers, owing to the stability and physical presence of a mixing layer on the surface, as a result of precipitation of corrosion products and presumed biofilm formation. This finding corroborates the OCP biofilm transition from initiation to growth stage. The EC representation for this system can be described by Figure 3a and 3b; the first days include an activation capacitance RC analog, and after 25 days, two time constants are represented by two constant phase elements.

3.2.1 Zinc Rich Epoxy

The EIS results for the ZnR sample are shown in Figure 2(c) and 2(d). Two loops are observed: one at medium-high frequency and another at low frequency in the complex representation. In the phase angle representation, two time constants are observed, representing the interfaces due to the presence of a mixed layer (biofilm, epoxy coating) and the zinc particle/coating interface. Figure 3b represents the equivalent circuit used for the ZnR epoxy/steel interface in the early stage. Part of this circuit has been proposed by Cubides to represent the ZnR on a metallic substrate system when the zinc particles are active after being exposed to an electrolyte, where R_s is the electrolyte resistance, R_p is the porous layer resistance formed by the coating, CPE_1 is the constant element for medium frequencies, R_{ct} is the charge transfer resistance due to the active particle/coating interface, CPE_2 is the constant phase element associated with the double layer capacitance, and n is the roughness factor. (Cubides and Castaneda, 2016). In general, all the impedances are higher than those of the bare steel samples, as can be seen in Table 2. This is due to conductivity of the Zn-rich epoxy influenced by the polymer coating matrix. In addition, the impedance signal is influenced by several factors such as electrolyte uptake within the coating, the galvanic effect of the Zn particles, the relation between Fe/Zn areas exposed to electrolyte, product formation, and biofilm formation (Abreu et al., 1999; Galicia et al., 2017). The R_{ct} impedances in this case are within an order of magnitude at around 50,000–100,000 Ω-cm^2 as illustrated in Table 2. This is in concordance with the OCP results in which the behavior of the systems is maintained at a specific potential zone. The semicircle acquired at the higher-medium frequency is associated with presumable coating-biofilm mixed layer, and the semicircle recorded at low frequency is the response of Zn/Epoxy interfacial reactions. The equivalent circuits describing the early stage of the system are illustrated in Figure 3b. The EC shows two time constant phase elements in parallel with two resistances representing early and continued evolution for 20 days. The time constants associated with the medium and low frequencies are consistent with the evolution of each element in the system. During the initial days, the electrolyte uptakes the coating and wetting of Zn particles, even though the galvanic effect prevailing at the particle/coating interface the overall OCP shows positive magnitudes away from the cathodic protection potential for anaerobic conditions, this latter can be attributed to the poor particles interconnection within the epoxy, resulting in a small area for the electrochemical reaction. The zinc particles react to produce ionic species and corrosion products; the zinc ionic species preserve the surface of the coating with no biofilm formation, likely due to a cytotoxic mechanism against microorganisms (Babich and Stotzky, 1978, Billanger et.al., 2015, Tong et.al., 2015). Two time constants are maintained for the

phase angle representation while the R_p and R_{ct} impedance in the complex representation increases up to 20 days. The wetting of the zinc particles following the charge transfer reactions no longer predominates, owing to the formation of corrosion products such as ZnO and $Zn(OH)_2$ at the zinc particle/coating interface, as reported previously (Cubides et al., 2016). The production of extracellular polymeric substances (EPSs) apparently begins to influence the high impedance values revealed at high-medium frequencies. Subsequently, a mature biofilm forms a heterogeneous layer as illustrated in Figure 4(a) obtained by scanning electronic microscopy, SEM. After 20 days, the complex signature reaches a higher impedance magnitude, resulting in the capacitance EIS signature representation. This latter result is consistent with the phase angle representation with the formation of only one time constant at medium-low frequencies. The final layer is a mixture of EPS/biofilm, corrosion products and precipitates, which allows the capture of the influence of this layer in the frequency interval range. The phase angle identifies one time constant in the system with a magnitude of 60 degrees, closer to the ideal capacitor effect of 90 degrees. This latter is attributed to a semi compact (heterogeneous) layer formed by mixture of organic epoxy, organic EPS/biofilm and corrosion products. The sample was evaluated at 29 days of bioelectrolyte exposure conditions. The Zn-rich epoxy illustrated in Figure 4(a) shows that the morphology is modified after exposure and demonstrates the underlying mechanisms; the sample shows the presence of a heterogeneous Extracellular Polymeric substances on the electrode as a biofilm. The balance between the Zn presence and the biofilm formation produce a biolayer of 12.5 µm in thickness.

3.2.2 Zinc Rich Epoxy with 1CNT

The Nyquist diagram of the Zn-1CNT is displayed in Figure 2(e) for the complex representation and 2(f) for the phase angle. There is one loop with a finite locus point in the real axis, owing to the capacitance behavior and charge transfer reaction step control process at the zinc/coating interface. At day 5, the R_{ct} impedance magnitudes in the EIS signature are similar in magnitude to those of the ZnR epoxy samples. The electrical interconnection between Zn particles is increased with the addition of CNTs, which in turn favors the formation of products within the coating through favoring the charge transfer reaction at the Zn/coating interface, and the level of protection subsequently improves, as corroborated by the OCP in early stages. The presence of the CNTs promoted zinc particle area/substrate or particle/particle interactions; initially, charge transfer process kinetics are favored due to the area available for galvanic reactions. The initial presence and distribution of extracellular polymeric substances was influence by Zn leaching and precipitation within the coating as well as precipitation at the surface of the corrosion products. EPS formation and subsequent biofilm stability was influenced by the amount of reacted zinc at the particle/coating interface. Following system evolution, changes in the corrosion products and growth of the biofilm shifted the charge transfer magnitude. Competition between formation of the biofilm on the surface and the corrosion products within the coating is balanced by the formation of zinc ions and influenced by the amount of CNTs. The SEM image in Figure 4(b) shows a smaller biofilm thickness on the coating surface after 29 days of exposure when the concentration of CNTs stayed at 1CNT. The impedance gain could mark a transition moment of the system, which does not follow the EIS application principle of stability (Bosch et al., 2001) because the OCP for the sample decreased significantly at 10 days. However, the subsequent

exposure times at 15, 20, and 25 days exhibit an increase in charge transfer resistance, or R_{ct}, which agrees with the OCP results. The 1CNT concentration influences the EPS, biofilm formation and mix layer, by dissolution or inhibition mediated by the Zn ions and the kinetics of the corrosion products formed at the Zn particle interface. This latter result is due to the decrease in Zn ionic formation caused by surface de-activation of particles and their depletion resulting from their usage in the formation of corrosion products, with the decrease also due to biofilm inhibition (Babich and Stotzky, 1978, Bong et al., 2010). The presence of one time constant in the phase angle representation for Zn-1CNT reflects the influence of capacitive behavior resulting from a mixture of the organic coating, inorganic corrosion products and biofilm. This indicates that a mix layer was formed on top of the coating, as evidenced by the impedance signature of Figure 2(f) and SEM image of Figure 4(b). The morphology of the biofilm is very different from that of with zinc-rich sample. The Zn products were obtained with a higher density, the corrosion products expanded the ZnR coating in some locations, and the biofilm was no continuous compared with ZnR. For Zn-1CNT, the phase angle shows one-time constant appearance at early stage. The early stage at OCP correlates interconnectivity of the CNTs, with active zinc particles reacting faster compared to without the CNTs

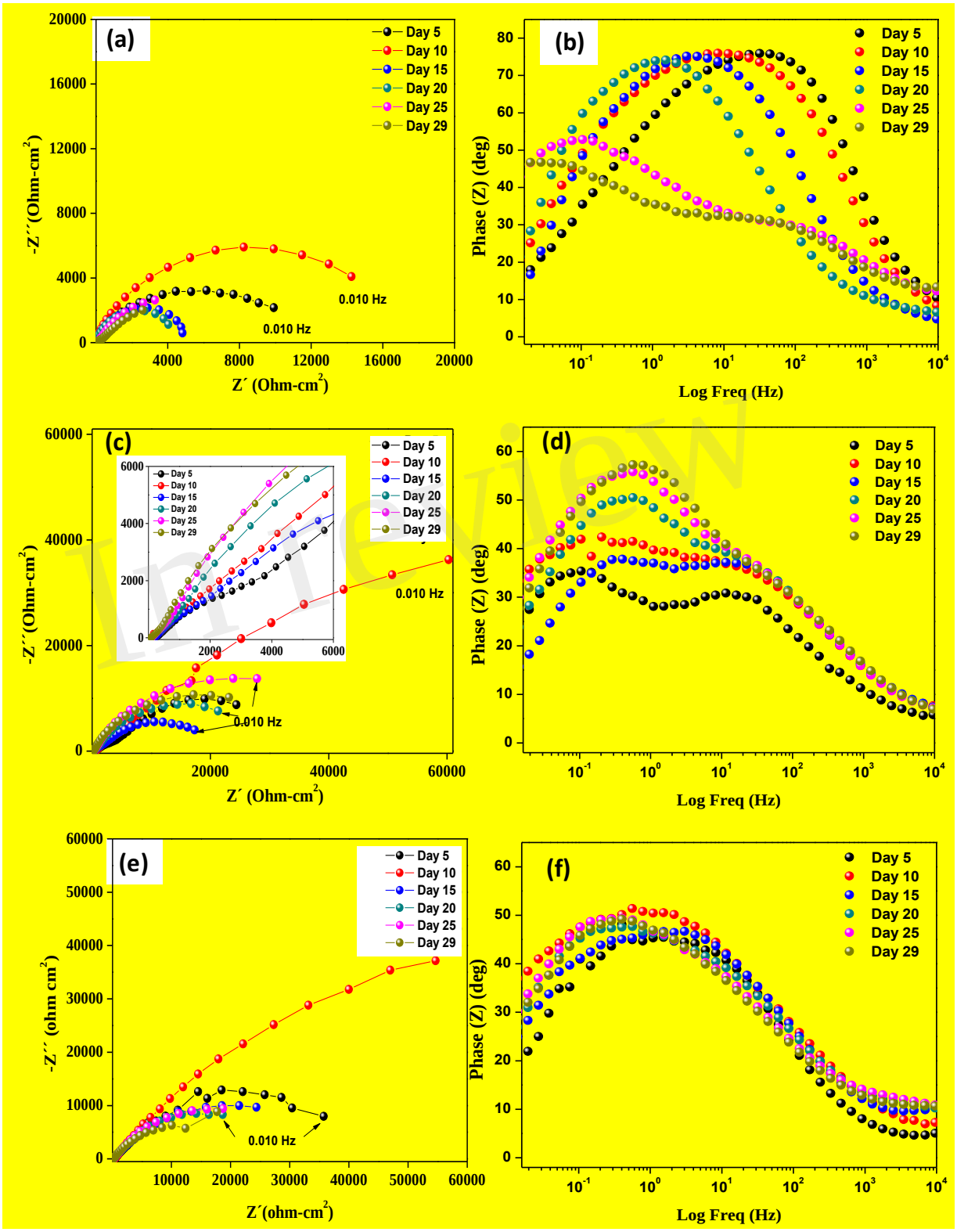

Fig. 2. Diagrams of Nyquist and phase angle in the SRM consortium for (a)-(b) 1008 bare steel, (c)-(d) for ZnR coating, and (e)-(f) for Zn-1CNT coating.

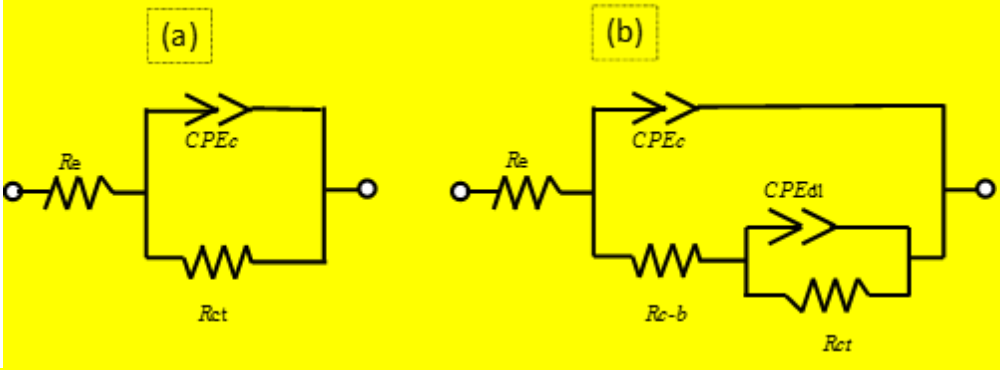

Fig. 3. Equivalent circuits proposed for the interface evolution on the basis of the interfacial components

Table 2

Fitting parameters from an equivalent circuit simulation for AISI 1008 bare steel

Circuit element → Time (day) ↓	R_e ($\Omega \cdot cm^2$)	CPE_1 ($F\ cm^{-2}$)	α	$Rc\text{-}b$ ($\Omega \cdot cm^2$)	CPE_2 ($F\ cm^{-2}$)	R_{ct} ($\Omega \cdot cm^2$)
5	4.7	1.5E-04	.8	-	-	11987
10	5.0	1.7E-04	.8	-	-	15090
15	5.7	4.2E-04	.8	-	-	5254
20	7.1	8.6E-04	.8	-	-	5137
25	9	7.1E-04	.5	315	4.1E-04	16554
29	22	1.7E-05	.5	977	8.7E-04	12352

Table 3

Fitting parameters from an equivalent circuit simulation for multifunctional coatings

Circuit element → Time (day) ↓	R_e ($\Omega \cdot cm^2$)	CPE_1 ($F\ cm^{-2}$)	α	$Rc\text{-}b$ ($\Omega \cdot cm^2$)	CPE_2 ($F\ cm^{-2}$)	R_{ct} ($\Omega \cdot cm^2$)
ZnR						
5	502	8.5E-07	.5	21204	5.7E-07	39143
10	400	4.6E-07	.5	175716	6.8E-07	53761
15	205	9.8E-07	.5	23631	1.3E-06	1203
20	171	1.2E-04	.6	29509	5.8E-07	5654
25	138	1.1E-04	.7	-	-	29245
29	85	2.1E-04	.7	-	-	26936
Zn-1CNT						
5	400	8.9E-07	.6	-	-	39001
10	426	5.4 E-07	.6	-	-	50038
15	183	1.0E-02	.6	-	-	37817
20	139	1.4 E-02	.6	-	-	33855
25	132	1.6 E-02	.6	-	-	39595
29	109	2.2 E-02	.6	-	-	39516
Zn-2CNT						

5	290	5.0E-07	.6	-	-	77908
10	157	1.0E-05	.6	-	-	35247
15	125	6.7E-05	.6	-	-	43741
20	123	7.2E-05	.6	-	-	42736
25	138	9.2E-05	.6	-	-	43580
29	49	3.1E-04	.6	-	-	13532

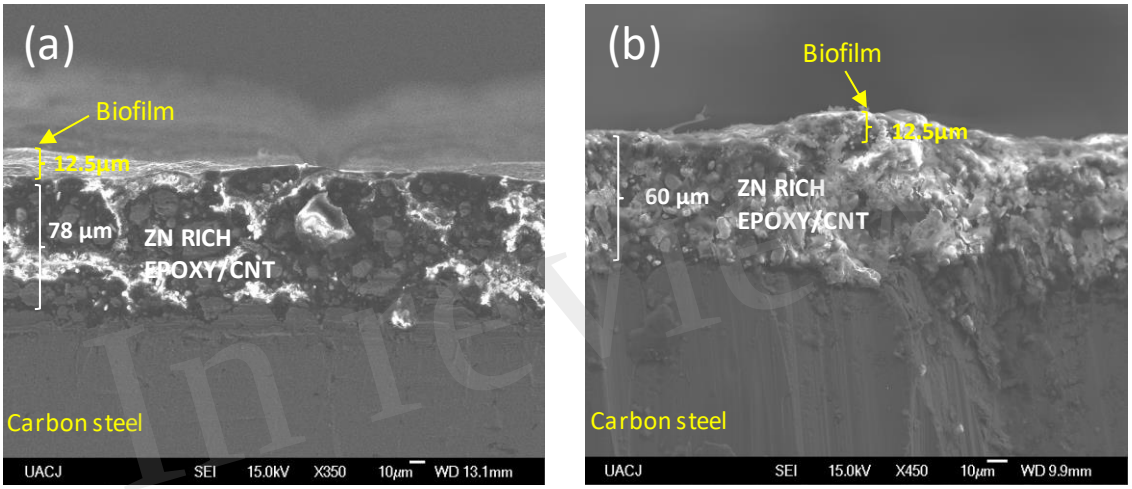

Fig. 4. Cross-section SEM images of the coatings immersed in an electrolyte with the SRM consortium. (a) Zn rich-primer, (b) Zn-rich primer with 1 wt.% CNTs

3.2.3 Zinc Rich Epoxy with 2 CNT

The impedance signature of the Zn-2CNT sample is exhibited in Figure 5(a) and 5(b). There is one loop for the complex representation and one time constant for the phase angle signature. The electrical connection among the Zn particles is evident in the OCP results, and this is associated with a Zn area that is much greater than the Fe iron exposed to the electrolyte, which is due to the increased CNTs content. The EIS signature corroborates the formation/initiation of EPS and the biofilm as well as the charge transfer dominance due to Zn particle activation, resulting in corrosion products within the coating. The formation of corrosion products at the particle/coating interface should be favored due to the higher electronic interconnectivity. However, the biofilm does not form homogeneously due to the presence of Zn products formed from bulk zinc ion generation from the coating and their transport to the coating surface. The substantial CNT content surpasses the ionic Zn content that inhibits biofilm formation. After 10 days, the impedance magnitude decreases, owing to the activation of Zn particles. At day 29, the system evolves to the lowest charge transfer resistance, R_{ct} magnitude. The CNT increases the Zn particle kinetics and avoids continuous formation of a mixed layer that does not appear at this concentration.

The impedance analysis gave insight into the competition among anodic dissolution of zinc particles, EPS/biofilm formation, and the formation of zinc-rich corrosion products. Phase angle representation shows one time constant. The signature is characteristic of capacitive process and controlled by charge transfer resistance. The time constant at medium frequencies may represent the influence of a capacitance of a unified (mixed) layer forming at the surface, and the low frequency characterizes the particle/coating interface. With time, anodic dissolution of Zn and the formation of Zn corrosion products become less prevalent, and thus do not provide sufficient protection to the metal substrate. From the Nyquist plot, the impedance of the ZnR coating increased with time. Great influence in resistance is attributed to the EPS/biofilm formation noted above in combination with inorganic semiconductor ZnO and $Zn(OH)_2$ corrosion products following Zn dissolution, which provides added barrier. EIS analysis agrees with the OCP measurement findings in that the addition of CNTs to the polymeric matrix structure improves the electrical connectivity between zinc particles and the metallic steel substrate through electron transport. In early stages, both the Zn-1CNT and Zn-2CNT coated samples showed potential below the CP threshold potential. SEM images after 28 days of immersion in Figure 7, suggest that the biofilm forms at the early days of immersion and subsequently grows/inhibits based on the Zn content generated by the more efficient galvanic system. The limited presence of an exopolysaccharide matrix, along with the limited population of bacteria and other organisms, accounts for the possibility that biofilm limited formation at the surface occurred, in part due to the presence of carbon nanotubes for Zn-1CNT and Zn-2CNT.

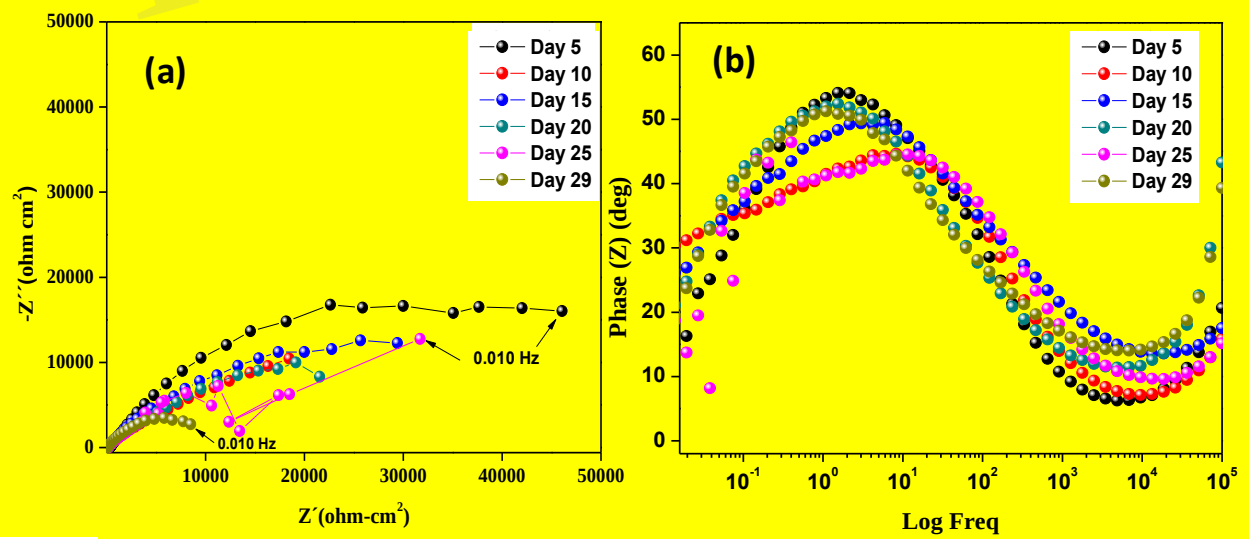

Fig. 5. Diagram of Zn-2CNT coating in the SRM consortium: Nyquist (a) and phase angle (b) representations.

The SEM image of a Zn-2CNT sample in Figure 6 shows several regions with biolayer removal and some residual Zn particles in the epoxy. This Zn-2CNT sample has the thinnest randomly distributed biofilm formed at the top of the coating surface. This latter result, could be attributed to the dissolution of zinc particles, which form $ZnCl_2$ or ZnO that presumably inhibit initial biofilm

formation by poisoning certain cellular elements present in microorganisms (Tong et al.). Many investigations have demonstrated that zinc cations, zinc oxides and zinc chlorides are cytotoxic by disturbing gene regulation processes associated with the production of extracellular polymeric substances (EPSs) (Babich and Stotzky, 1978, Billanger et.al., 2015, Tong et.al., 2015). The above factors prevent construction of the matrix component of the biofilm. OCP and EIS results were able to demonstrate initiation of the biofilm or mixed layer formation due to the transient state revealed by both techniques over time. The shifts in OCP, magnitude and impedance elements associated with the system interfaces accompanied trends including formation of the biofilm is a clear indicator of the influence by the CNT in terms of corrosion control mechanism. Zn ions formed following CNT addition, which are then transported into the coating and inhibit biofilm formation in locations with a higher density of Zn particles, the Zn and CNT content can be balance to establish a critical magnitude or Zn/CNT ratio for the efficiency of the ZRE epoxy coatings.

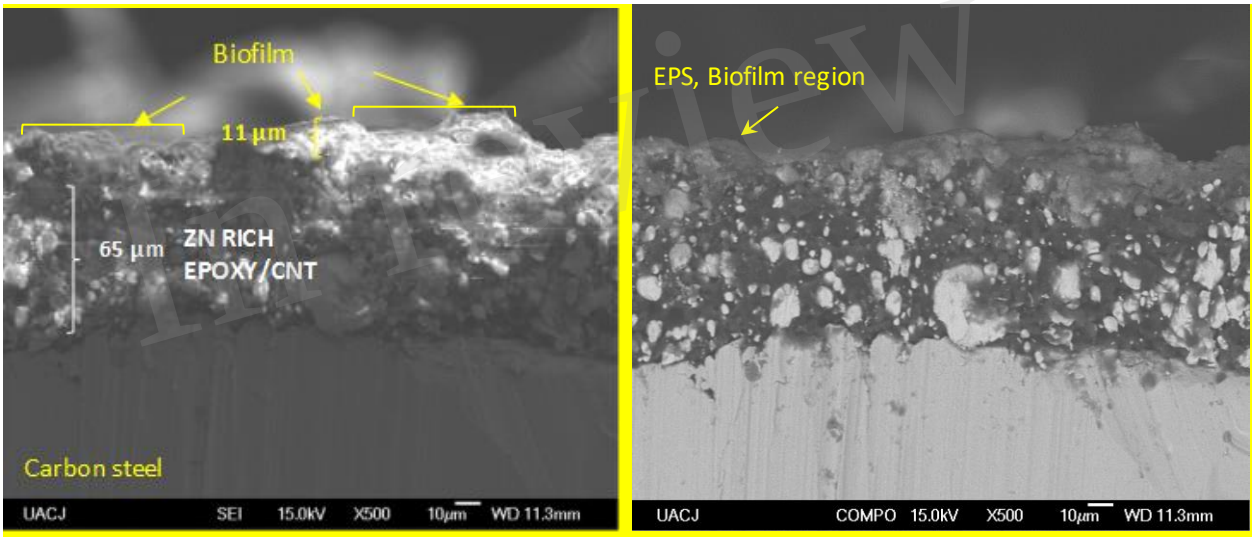

Fig. 6. Cross-sectional SEM images of the coatings immersed in an electrolyte with the SRM consortium. Zn-rich primer with 2 wt.% CNTs. Morphology of the image and a back scattered electron image.

3.3 Surface evolution (top and cross section) characterization before and after bioelectrolyte exposure

Figure 7 shows the cross-section SEM images obtained for the multifunctional coatings after 29 days of immersion in the SRM bioelectrolyte. These images corroborate the findings from the OCP data and the impedance analysis. For Zn-1CNT and Zn-2CNT coatings, it was possible to detect and demonstrate the presence and interconnectivity of Zn particles with carbon nanotubes at the interface of carbon steel, the coating matrix itself and the EPS/corrosion product layer. The biofilm layer can be considered to provide greater extension for the ZnR coating because, as described above, the CNT content leads to cytotoxicity toward the main bacterial and fungal constituents of

the SRM consortium (Upadhyayula and Gadhamshetty, 2010). The increase in CNT content promotes the formation of Zn ions, thus resulting in a cytotoxic environment. The images in Figure 7 reveal biofilm patch formation instead of a continuous layer at the electrode surface. Therefore, the presence of biofilm is not favored when CNTs are present.

The presence of CNTs, as evident in Figure 7, was associated with an excellent influence on conductivity at the inner section of the coating according to the impedance analysis. Lack of uniform layer is ascribable to the dissolution of zinc cations, which are presumably cytotoxic to the microorganisms. In turn, zinc ions could be also responsible for the formation of corrosion products such as ZnO and $ZnCl_2$, also the presence of these corrosion products also became evident according to the EDS elemental analysis, this latter illustrated in Figure 8.

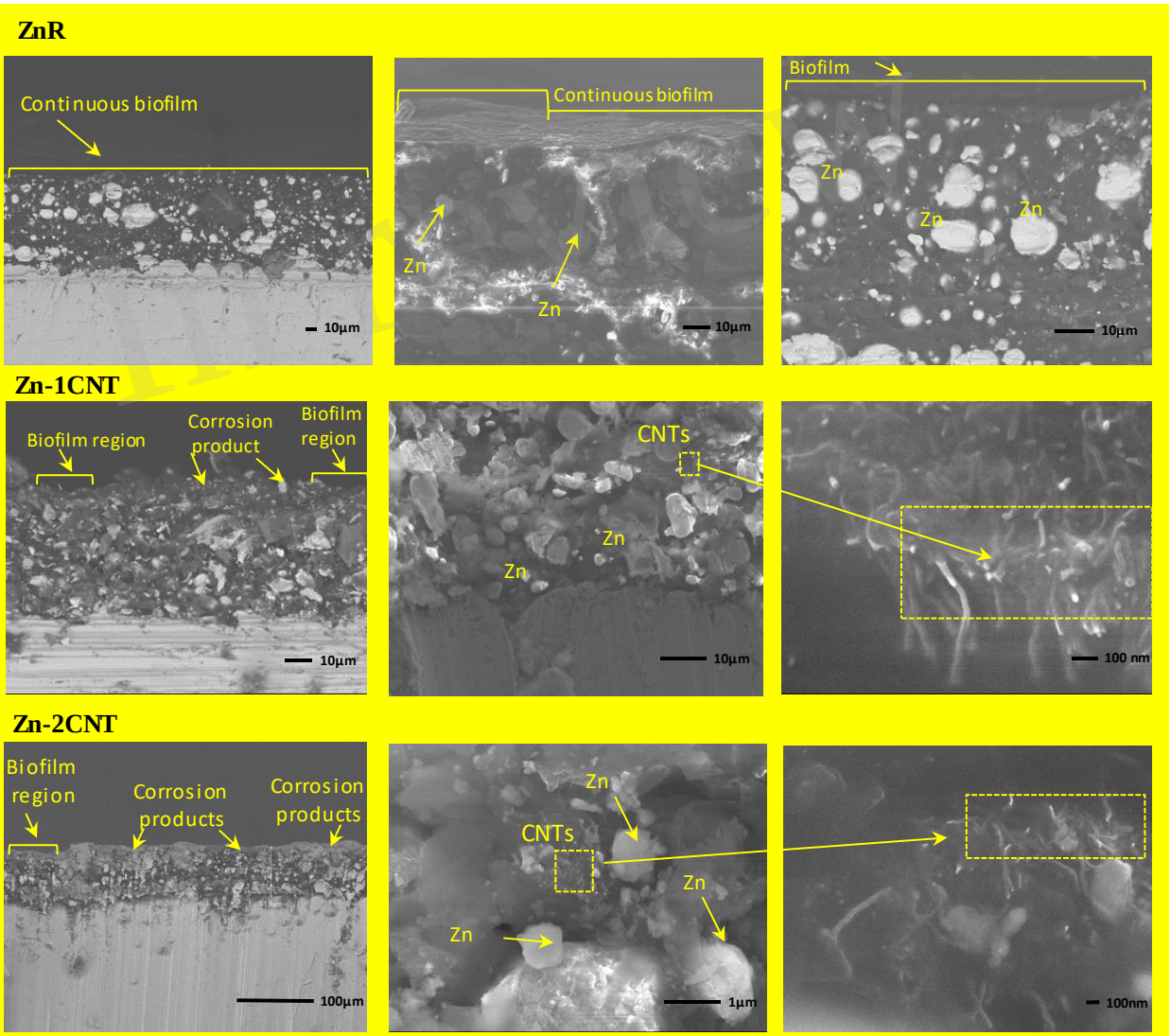

Fig. 7. Cross-section SEM images of the multifunctional coatings immersed in an electrolyte solution with the SRM consortium: Zn rich-primer, Zn-rich primer with 1 wt.% CNTs and Zn-rich primer with 2 wt.% CNTs.

Figure 8(a) to Figure 8(c) show top-view SEM images of the three multifunctional coatings after 29 days of immersion in bioelectrolyte. For ZnR in Figure 8(a), a continuous layer of extracellular polymeric substances is observed covering the surface, which becomes less evident in the presence of CNT particles. Figure 8(b) illustrates the initial formation and lack of persistence of a layer of biofilm that shows some heterogeneous and residual over time. This finding is attributable to the inhibition of mature biofilm formation by the CNTs influence along with a poisoning mechanism by the cytotoxic effect of Zn soluble products (Babich and Stotzky, 1978, Bong et al.) At this respect, CNTs are considered to have adverse effects on biofilm growth at some levels according to the investigations of Upadhyayula and Gadhamshetty (Upadhyayula and Gadhamshetty, 2010). When a double content of CNTs is present, a greater porosity can be appreciated as shown in Figure 8(c), which is mainly attributed to the lack of continuous biofilm layer caused by an increased level of zinc corrosion products and the double content of carbon nanotubes that alter the development and formation of a mature biofilm.

Also, Figure 8(a)-8(c) show the EDS analysis demonstrating that the ZnR coating has a higher content of organic compounds, such as carbon, sulfur, nitrogen, and phosphorous (C, S, N and P) due to presence of a more mature biofilm, which supports the OCP data and impedance results. For the Zn-1CNT and Zn-2CNT coatings, a higher content of Zn and O is evident, and a lower level of organic compounds is found. Higher Zn levels indicate the formation of zinc corrosion products over the coating surface. In addition, the Zn-1CNT and Zn-2CNT coatings exhibit higher Zn and O content, thus further indicating that these coatings inhibit the formation of extracellular polymeric substances (Babich and Stotzky, 1978, Bong et al., 2010, Billanger et al., 2015, Tong et al., 2015), and therefore disturb biofilm growth to a greater extent due to the toxicity of the high levels of CNTs (Upadhyayula and Gadhamshetty, 2010).

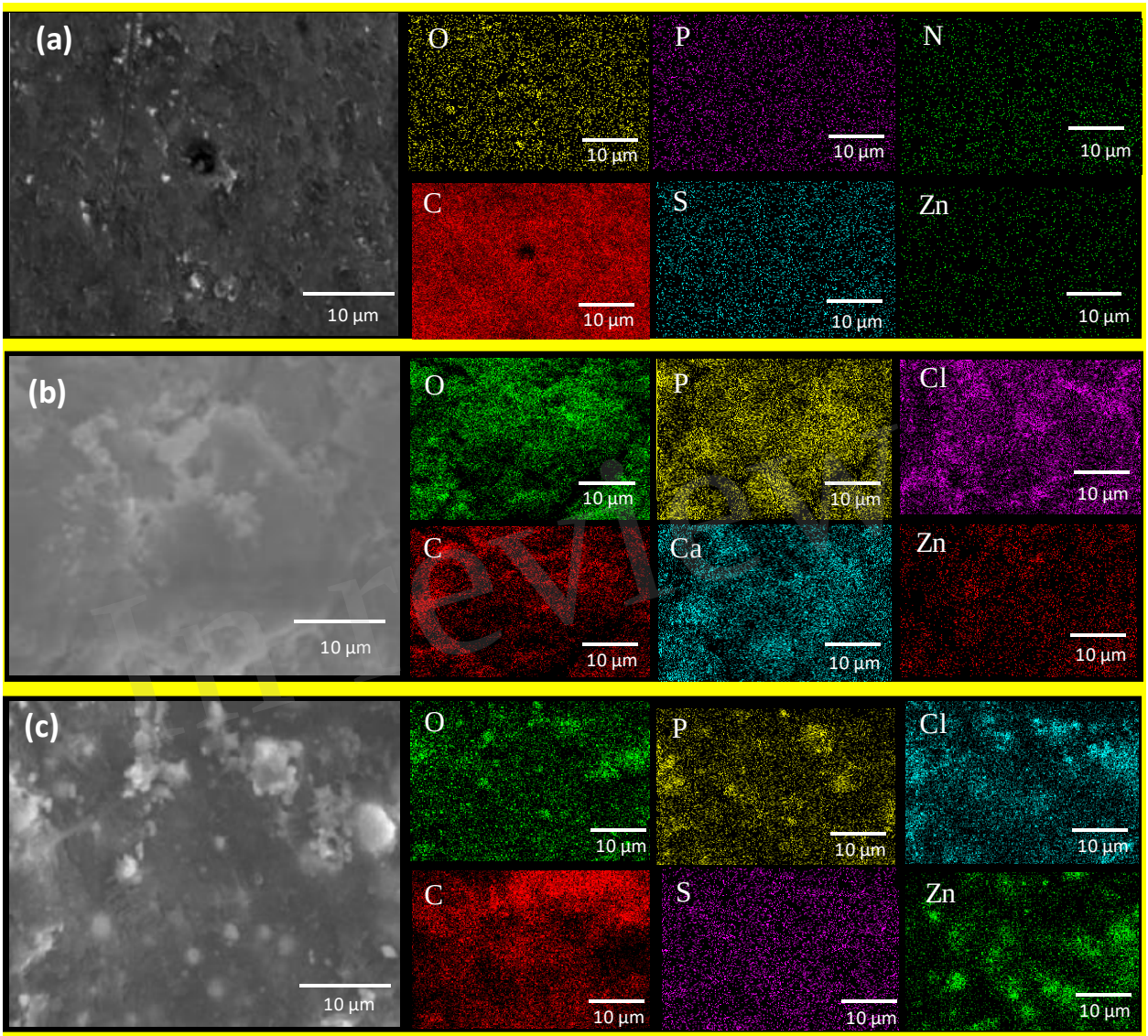

Fig. 8. Top views and EDS mapping analysis showing coatings samples after 29 days of exposure to the SRM consortium, (a) ZnR, (b) Zn-1CNT, and (c) Zn-2CNT. ZnR coating has a high content of organic compounds, such as carbon, sulfur, nitrogen and phosphorous (C, S, N and P) due to biofilm formation.

4 Conclusions

This investigation determined that for these multifunctional coatings, the anodic dissolution of zinc particles, the formation of an extra biolayer and the formation of zinc-rich corrosion products represent competing processes. The contribution of an extra layer formed on the coating surface can be attributed to the formation of EPSs and a biofilm by the SRM consortium. The CNTs content enhances the anodic reactions of the zinc particles in the coatings, promoting cathodic

protection and the formation of more corrosion products in the form of solid oxide/hydroxide compounds. However, doubling the CNT content results in more interaction with the zinc particles and impairment of biofilm growth. This represented a qualitative influence of CNTs concentration as evidenced by reduced levels of corrosion products. The ZnR coating exhibits galvanic protection, as evidenced by the formation of corrosion products and secretion of extracellular polymeric substances to produce a more homogeneous biolayer. The Zn-1CNT coating exhibits partial cytotoxicity towards microorganisms, thereby controlling biofilm initiation and growing processes. The Zn-2CNT ratio represents the saturated concentration of carbon nanotubes leading to less-optimal conditions for biofilm formation. Finally, we considered to be a CNTs content that could be used to balance biofilm formation and zinc anodic dissolution to influence microbiologically induced corrosion mechanisms.

5 Acknowledgements

Monica Galicia would like to thank Ivan Salcido for assistance with SEM images. Also, the authors would like to thank QBP Graciela García for a culture donation, Ms. Violeta Valencia for the electrochemical set up design and Israel Barraza for valuable discussions.

6 References

Abdolahi A., Hamzah, E., Ibrahim Z., Hashim S. (2014). Application of Environmentally-Friendly Coatings Toward Inhibiting the Microbially Influenced Corrosion (MIC) of Steel: A Review. Polym. Rev. 54:4,702-745. doi:10.1080/15583724.2014.946188.

Abreu, C.M., Izquierdo, M., Perino P., Novoa X.R., Pérez, C. (1999). A New Approach to the Determination of the Cathodic Protection Period in Zinc-Rich Paints. Corrosion. 55,12:1173-1181. doi:10.5006/1.3283955.

Babich, H., and Stotzky, G., (1978) Toxicity of Zinc to Fungi, Bacteria, and Coliphages: Influence of Chloride Ions, Appl. Environ. Microbiol. 36: 6, 906-914.

Billanger, X., Billard, P., Schneider, R., Balan, L., Merlin, C. (2015). Stability and toxicity of ZnO quantumdots:Interplay between, nanoparticles and bacteria, J. Hazard Mater. 283, 110-116. Doi:.org/10.1016/j.jhazmat.2014.09.017.

Bong, C.W., Malfatti, F., Azam, F. Obayashi, Y., Suszuki, S. (2010) The Effect of Zinc Exposure on the Bacteria Abundance and Proteolytic Activity in Seawater, Interdisciplinary Studies on Environmental Chemistry — Biological Responses to Contaminants 57–63. © by TERRAPUB.

Bosch, R.W., Moons, F., Zheng, J.H., Bogaerts, W.F. (2001). Application of electrochemical impedance spectroscopy for monitoring stress corrosion cracking. Corrosion. 57,6: 532-539.doi:10.5006/1.3290379.

Castaneda, H. and Benetton X. (2008). SRB-biofilm influence in active corrosion sites formed at the steel-electrolyte interface when exposed to artificial seawater conditions. Corr Sci. 50, 4: 1169-1183. doi:10.1016/j.corsci.2007.11.032.

Ciubotariu A., Benea L., Sand W. (2015). Effects of sulphate reducing bacteria on thermosetting polymer-Zn composite coatings, "Mircea cel Batran" Naval Academy Scientific Bulletin, Vol. XVIII – 2015 – Issue 1 "Mircea cel Batran" Naval Academy Press, Constanta, Romania//PROQUEST SciTech Journals, PROQUEST Engineering Journals, Technology Journals, PROQUEST Military Collection PROQUEST Advanced Technologies & Aerospace.

Cubides Y., and Castaneda H. (2016). Corrosion protection mechanisms of carbon nanotube and zinc-rich epoxy primers on carbon steel in simulated concrete pore solutions in the presence of chloride ions, Corr. Sci. 109, 145-161. doi:10.1016/j.corsci.2016.03.023.

Deflorian F., Rossi, S., Fedrizzi, L., Bonora PL. (2005). EIS study of organic coating on zinc surface pretreated with environmentally friendly products, Progress in Organic Coatings 52: 4, 271-279.

Enning D., and Garrelfs J. (2014). Corrosion of Iron by Sulfate-Reducing Bacteria: New Views of an Old Problem, Appl. Environ. Microbiol. 80: 4, 1226-1236. doi:10.1128/AEM.02848-13.

Fedel, M., Rodríguez Gómez, FJ., Rossi, S., Deflorian, F. (2019). Characterization of Polyorganosilazane-Derived Hybrid Coatings for the Corrosion Protection of Mild Steel in Chloride Solution, Coatings 9: 10, 680.

Galicia, M., Valencia V., Aguirre-Ramírez., Castaneda, H. (2017). Interfacial and Corrosion Characterization of Zinc Rich-Epoxy Primers with Carbon Nanotubes Exposed to Marine Bacteria, in CORROSION 2017. 2017, NACE International: New Orleans, Louisiana, USA.

Guan, F., Zhai,X., Duan, J., Zhang, M. Hou, B. (2016). Influence of Sulfate-Reducing Bacteria on the Corrosion Behavior of High Strength Steel EQ70 under Cathodic Polarization. PLoS One, 11(9): e0162315. doi: 10.1371/journal.pone.0162315

Jeon, H., Park J., and Shon M. (2013). Corrosion protection by epoxy coating containing multi-walled carbon nanotubes. Journal of Industrial and Engineering Chemistry. 19(3) 849-853. doi:0.1016/j.jiec.2012.10.030.

Liu, D., Fe Lin, Q., Hui Li, C., Li Xue, L. (2007). Improvement of MIC Behavior of Low Alloy Steel with Zn-Rich Epoxy Coating. Key Engineering Materials, 348-349: 509-512. doi:10.4028/www.scientific.net/KEeM.348-349.509.

Liu T. and Cheng Y. F. (2017). The influence of cathodic protection potential on the biofilm formation and corrosion behaviour of an X70 steel pipeline in sulfate reducing bacteria media. Journal of Alloys and Compounds. 729: 180-188. doi: /10.1016/j.jallcom.2017.09.181 0925-8388

Park, SM., and Shon, MY. (2015). Effects of multi-walled carbon nanotubes on corrosion protection of zinc rich epoxy resin coating. Journal of Industrial and Engineering Chemistry. 21, 1258-1264. doi: 0.1016/j.jiec.2014.05.042.

Schwerdtfeger, Current and potential relation for the cathodic protection of steel in salt water. J. Research NBS GO, 153 (1958) RP2833; Corrosion 14, 446t (Oct. 1958).

Tong, T., Wilke, CM., Wu, J., Binh, CT., Kelly, JJ., Gaillard, JF., Gray, KA. (2015). Combined Toxicity of Nano-ZnO and Nano-TiO2: From Single- to Multinanomaterial Systems, Environ. Sci. Technol. 49, 8113−8123. doi: 10.1021/acs.est.5b02148.

Upadhyayula, V. and Gadhamshetty, V. (2010). Appreciating the role of carbon nanotube composites in preventing biofouling and promoting biofilms on material surfaces in environmental engineering: A review. Biotechnology Advances 28,6: 802-816.
doi: 10.1016/j.biotechadv.2010.06.006.

Wang J., Li Q-f., Fu Y-d., Li C-h. (2012). MIC Behavior of the Low Alloy Steel with Different Zn-Epoxy Coating in SRB Solution. Key. Eng. Mater. 488-489, 262-265. doi: 10.4028/www.scientific.net/KEM.488-489.262.

Wang, J., Fe Lin, Q., Dong Fu, Y., Hui Li, C. (2012). MIC Behavior of the Low Alloy Steel with Different Zn-Epoxy Coating in SRB Solution. Key Engineering Materials. 488-489: 262-265.doi: 10.4028/www.scientific.net/KEM.488-489.262.

Weinell, C.E., and Rasmussen, S.N. (2007). Advancement in zinc Rich epoxy primers for corrosion protection, in CORROSION 2007, NACE International: Nashville, Tennessee.

Supplementary Material

Graphs for Module of Impedance

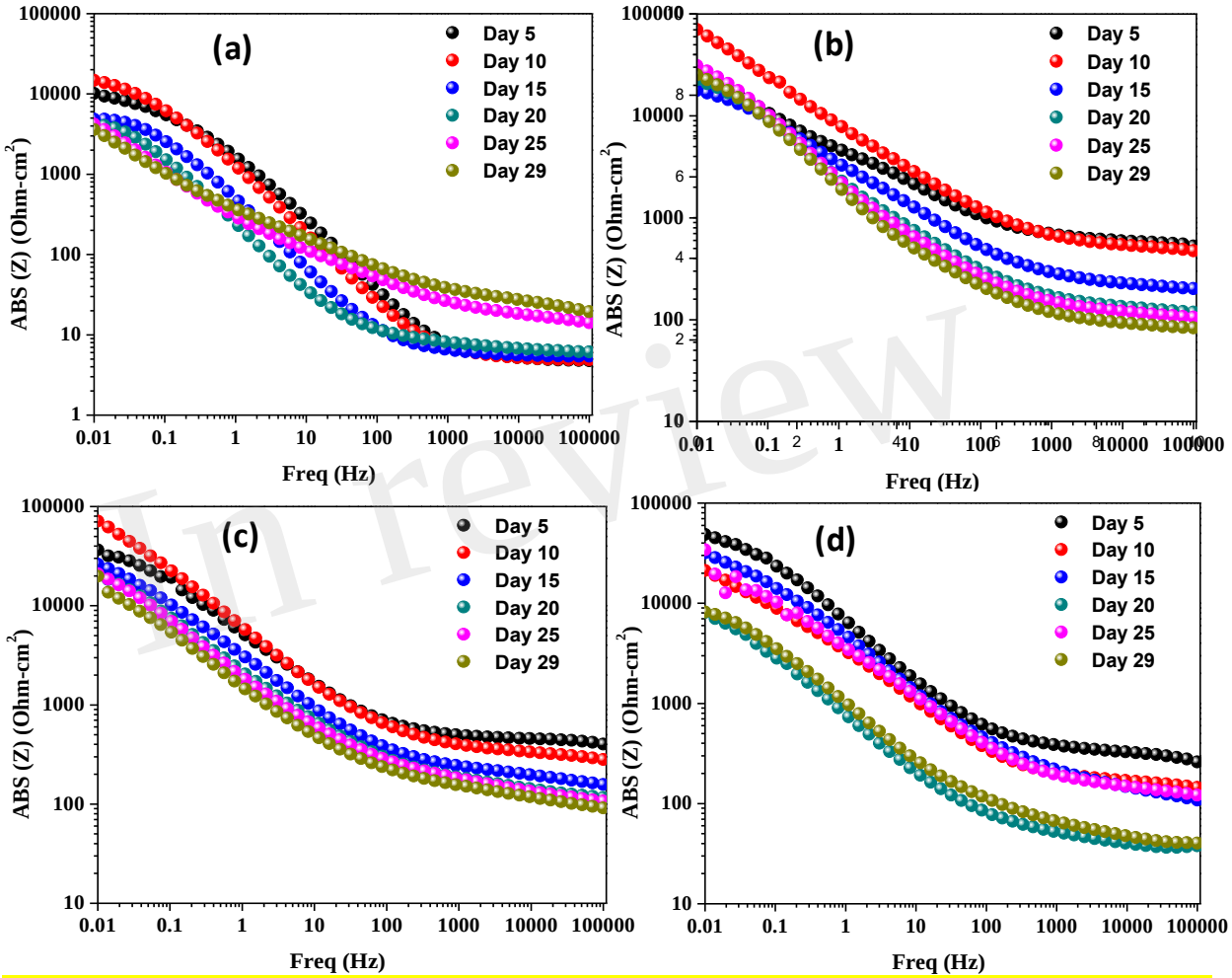

Diagrams of Module of Impedance in SRM consortium for (a)1008 Bare steel , (b)ZnR coating, (c)Zn-1CNT coating, and (d) Zn-2CNT coating.